Integration of solar latent heat storage towards optimal small-scale combined heat and power generation by Organic Rankine Cycle

Jesus Lizana [a*]
Chiara Bordin [b]
Talieh Rajabloo [c,d*]

[a] Instituto Universitario de Arquitectura y Ciencias de la Construcción, Universidad de Sevilla, Avda. Reina Mercedes 2, 41012 Seville, Spain
[b] Arctic University of Norway, Tromsø, Norway
[c] Hasselt University, Martelarenlaan 42, 3500, Hasselt, Belgium
[d] imec, Kapeldreef 75, 3000, Leuven, Belgium

* Corresponding author. E-mail address: flizana@us.es

* Co-corresponding author. E-mail address: talie.rajabloo@uhasselt.be

Abstract

Thermal energy and distributed electricity demand are continuously increased in areas poorly served by a centralized power grid. In many cases, the deployment of the electricity grid is not economically feasible. Small-scale Organic Rankine Cycle (ORC) appears as a promising technology that can be operated by solar energy, providing combined heat and power (CHP) generation. Additionally, thermal energy storage can ensure stable and continuous operation in case of scarce thermal energy availability. This paper evaluates the potential application of latent heat storage to enhance solar ORC performance at operating temperatures between 80ºC and 140ºC, aiming at improving the efficiency and capacity of ORC for low-cost non-concentrating solar-thermal collectors. Three thermal energy storage scenarios are considered. Scenario 1 and 2 consist of reference cases based on a solar ORC system integrated with a conventional hot water tank and a pressurised water tank. Scenario 3 implements a storage unit based on a phase change material. The simulation was carried out through models developed in TRNSYS for solar energy balance and ASPEN for ORC system performance. The results show that solar latent heat storage tank can provide 54% of useful collector gains with a higher and narrower temperature range in the evaporator, increasing the annual thermal energy capacity by 19%, reducing annual heat losses by 66% and decreasing the investment cost by 50% in comparison with a pressurised water tank. It also allows increasing the efficiency of ORC cycle by approximately 18% (from 8.9% to 10.5%) with a higher net generated power than a conventional water tank integration, scaled up from 498W to 1628W. These results highlight the potential benefits that latent heat integration provides to improve the low-cost solar ORC performance for powering electricity and thermal energy supply.

Keywords: Thermal energy storage; Solar thermal energy; Phase change material; ORC; Evacuated tube collector

Nomenclature

A	area, m^2
c_p	specific heat, KJ/(kg.K)
h	heat of fusion, kJ/kg
P	pressure, bar
Q	heat transfer rate, W
T	Temperature, ºC
ΔT	temperature difference, ºC

Abbreviations

CHP	combined heat and power
CSHP	combined solar heat and power
ETC	evacuated tube collectors
MCH	magnesium chloride hexahydrate
mt	melting temperature
ORC	Organic Rankine Cycle
PCM	phase change material
PV	photovoltaic
PVT	photovoltaic-thermal hybrid
TES	thermal energy storage

Subscript

cond	condensation
evap	evaporation
in	inlet
l	liquid
out	outdoor
s	solid

1. Introduction

Around 2 billion people worldwide do not have access to electricity. Typically, these populations live in remote areas far from the centralized electricity grids and are characterized by a low income. Besides, for electricity transmission and distribution operators, the deployment of electricity grids is not economically advantageous, as they prefer to extend their activities in urban areas [1].

In recent years, Organic Rankine Cycle (ORC) has attracted considerable attention in the scientific researches and appears as a promising technology for conversion of heat into electricity [2,3], since it can be designed for operation at low temperatures with suitably-selected working fluids [4]. The heat for ORC can be provided from various sources: solar radiation, biomass combustion, geothermal heat or waste heat from industry [5,6]. Hence, ORC would be an appropriate option for remote areas. For distant regions with a lot of sunshine, a combination of ORC and photovoltaic panels (PV) can be a suitable alternative for electricity generation. Furthermore, a tailored model and fine management can provide both electricity and thermal energy for the local inhabitants. An overview of the ORC market evolution, considering the present installed capacity, historical data and macro-economic trends, was reported by Tartière et al. [7]. They highlighted the future perspectives and growth potential of the ORC market by putting a special focus on waste heat recovery applications.

As a heat conversion technology, ORC is particularly suitable to increase the supply of renewable energy, mainly because of its ability to recover low-grade heat and the possibility to be implemented in decentralised low-capacity power plants [8]. A techno-economic survey of ORC systems was developed by Quoilin et al. [8], where was described as the state of the ORC technology with a particular emphasis on the temperature levels. In this study, a comparison with the traditional steam cycle revealed that ORC cycles are more appropriate for moderate power ranges and/or for low-temperature applications. Also, a compilation of the available market data showed that actual plant size is limited principally by a minimum power output of a few hundreds of kWe.

For small-scale power range, there is no commercial solution developed of ORC systems. Low-capacity systems are currently under development or in the demonstration phase because they still require attractive markets to begin industrial production and reduce their cost [8]. Rahbar et al. [9] carried out a review of ORC for small scale applications, with a focus on ORC configurations, applications, working fluid selection, modelling and experimental study of the expansion devices. The results highlighted that most studies carried out about the ORC were mainly devoted to the selection of suitable working fluids for various applications, thermodynamic modelling and optimization of the ORC performance metrics. Manolakos et al. [10] studied a 2 kWe low-temperature solar ORC with R134a as a working fluid and evacuated tube collectors. An overall efficiency below 4% was obtained. Wang et al. [11] studied a 1.6 kWe solar ORC using a rolling piston expander giving an overall efficiency of 4.2%. Kane [12] developed a model of a cascaded ORC using scroll expanders and coupled to a collector model.

The ORC integration is also being explored as an alternative to photovoltaic (PV) systems. Freeman et al. [13] investigated the heating and power potential of a small-scale combined solar heat and power (CSHP) system based on an ORC for domestic use in the UK, in comparison with a PV-thermal hybrid (PVT) system (producing electricity and hot water). The cost per unit generating capacity of a CSHP-ORC system is found higher than a PVT system. However, the authors highlighted that the PVT alternative has a significantly reduced capacity for hot water provision.

Small-scale solar organic cycles are well adapted for remote off-grid areas of developing countries. The performance and design optimization of a low-cost solar ORC for remote power generation was investigated by Quoilin et al. [14], showing that an overall electrical efficiency between 7% and 8% can be reached with conservative hypotheses.

The main benefit of ORC power unit is that it can operate using “freely” available thermal energy obtained from renewables, that can be stored. Thus, storage is a key issue in solar ORC systems, since the implementation of thermal energy storage (TES) is arguably a key advantage over systems based on PV technologies [15]. TES can ensure stable and continuous operation in case of scarce solar radiation and enables dispatchability in the generation of electricity and home space heating requirements.

Among the available TES alternatives, latent TES systems have recently received attention in the literature for ORC assemblies [4], as it is a more attractive solution than sensible storage because of the advantages of higher energy storage with a given volume, compactness and isothermal phase change [16]. Potential phase change material (PCM) candidates have demonstrated good performance for solar TES [17,18], showing benefits related to longer storage periods, reduced heat losses [19], and higher storage capacity for heating and hot water applications [20]. Bhagat et al. [21] developed a numerical analysis of latent heat TES using encapsulated PCM for a solar thermal power plant. It was found that the ability of the latent heat TES system to store and release energy is significantly improved by increasing mass flow rate and inlet charging temperature. Costa et al. [22] presented a solar salt latent heat thermal storage for a small ORC plant, operating at temperature levels between 220-230°C. Numerical simulations indicated that the use of metal foams provide the required thermal performance. Cioccolanti et al. [23] proposed an innovative small-scale concentrated solar 2 kWe ORC plant coupled with a PCM tank equipped with reversible heat pipes. The work represents a general guide for the design and optimization of the mutual interactions of the different subsystems in small-scale concentrated solar ORC plants.

Despite reported studies, efficiency numbers found in the literature of TES applications in ORC systems, at appropriate operating temperatures for the use of low-cost non-concentrating solar-thermal collectors, are reduced. Relevant studies must be accomplished to find an attractive solution for the PCM integration towards low-cost solar ORC configurations [24]. Aiming at overcoming the reported issues and defining criteria and strategies for the effective implementation of low-cost solar ORC units, this paper evaluates the performance of a small-scale solar ORC system integrated with evacuated tube collectors through three TES alternatives, two based on sensible storage and one in latent heat storage, with operating temperatures between 80ºC and 140ºC. The objective is to identify potential benefits and provide design criteria towards an optimal PCM implementation into low-cost solar ORC systems. Sensible heat storage alternatives consist of reference cases based on a conventional hot water tank and a pressurised water tank. They are compared with a latent heat storage unit, which implements a salt hydrate able to maximize the performance of ORC by storing and supplying high thermal energy amounts within a narrower and higher temperature range. Magnesium chloride hexahydrate was selected for the analysis due to a combination of favourable properties, such as high TES density, low-cost, availability and an appropriate melting temperature at 116ºC. The simulation was carried out through two models, developed in TRNSYS for solar energy balance and ASPEN for ORC system performance.

The paper is structured as follows. First, the methodology for simulation is detailed. This was divided into two stages: solar energy balance in TRNSYS and ORC model in ASPEN. Second, the results of three schematic assemblies for solar ORC systems are compared. Finally, the viability of solar ORC alternatives is discussed.

2. Methodology for numerical simulation

The performance of small-scale solar ORC system is evaluated through three TES scenarios, characterised in Table 1. Scenario 1 and 2 consist of reference cases based on a solar ORC system integrated with a conventional hot water tank and a pressurised water tank, as sensible TES units. Scenario 3 implements a PCM tank based on magnesium chloride hexahydrate (MCH), a latent heat storage material with a melting temperature of 116ºC. Three storage tanks have the same TES capacity for a temperature difference of 20ºC.

Table 1. Characteristics of three TES scenarios for small-scale solar ORC system.

Characterisation	Scenario 1: Water tank	Scenario 2: Pressurised water tank	Scenario 3: PCM tank
Storage medium	Water	Water	MCH
Storage temperature (ºC)	80-100ºC	110-130ºC	110-130ºC (mt at 116ºC)
Size (dm^3)	750	750	200
Tank height (m)	1.85	1.85	1.15
TES capacity (kWh)[a]	17.3 (80-100ºC)	17.3 (110-130ºC)	17.3 (110-130ºC)
Fluid specific heat (kJ/kg.K)	4.19	4.19	2.0/2.4 (solid/liquid)
Loss coefficient ($W/m^2.K$)	0.7	0.7	0.7
Q_{loss} (kWh/24h)[b]	≈6.38	≈8.77	≈2.93
Tank pressure (bar)	1.0-3.0	>5.0	-

[a] Storage capacity for a temperature difference of 20ºC.
[b] Considering 24h temperature decay from 100ºC for scenario 1, and from 130ºC for scenario 2 and 3, with an ambient temperature of 20ºC.

The numerical simulation was carried out through two models, developed in TRNSYS (Transient System Simulation) v18 [25] and ASPEN Plus simulation software [26], whose global schematic diagram is illustrated in Fig. 1.

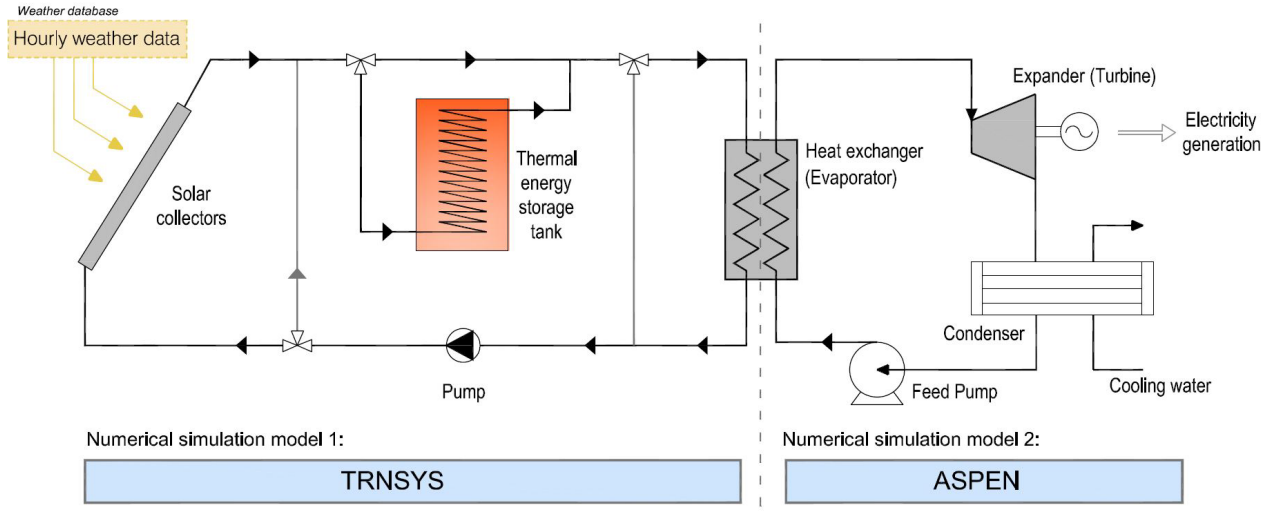

Figure 1. Schematic diagram of solar-ORC system with thermal energy storage.

TRNSYS was used for the assessment of solar energy balance. It is a flowsheet simulator with a graphical interface which facilitates the decomposition of complex problems into various, interconnected model components. TRNSYS implements algebraic and first-order ordinary differential equations, describing physical components into software subroutines (called Types), with a standard interface. The TRNSYS model library includes components for the calculation of solar systems, thermal energy storage units or building thermal loads, most of them experimentally validated, as well as climatic data files, which make it a very suitable tool for a reliable energy modelling.

ASPEN was used for the evaluation of ORC unit, using a validated ORC model previously reported in [27]. In this way, predefined components are settled in a close loop and simulation is done by defining required parameters, assumptions and strategies. Thermodynamic calculations through the program result in the amount of generated electricity. Then, cycle efficiency is calculated based on the results. Moreover, additional components are designed, integrated and analysed according to different requirements and alternative boundary conditions.

Both numerical simulations were carried out separately, without a direct coupling. The results of the solar energy obtained in TRNSYS (Step 1) were implemented as input data in the ASPEN model (Step 2) to analyse the potential benefits and drawbacks of two solar ORC integrations. Pipe heat losses have been neglected in all scenarios. In the next subsections, the simulation procedures used in each energy model are further described.

2.1. Solar energy balance

The evaluation of solar energy balance involves seven main components: weather data, solar collector, thermal energy storage, ORC heat exchanger, pump and controller. Fig. 2 and 3 illustrate the two proposed scenarios of small-scale solar ORC system based on water tanks (scenario 1 and scenario 2) and PCM tank (scenario 3), respectively.

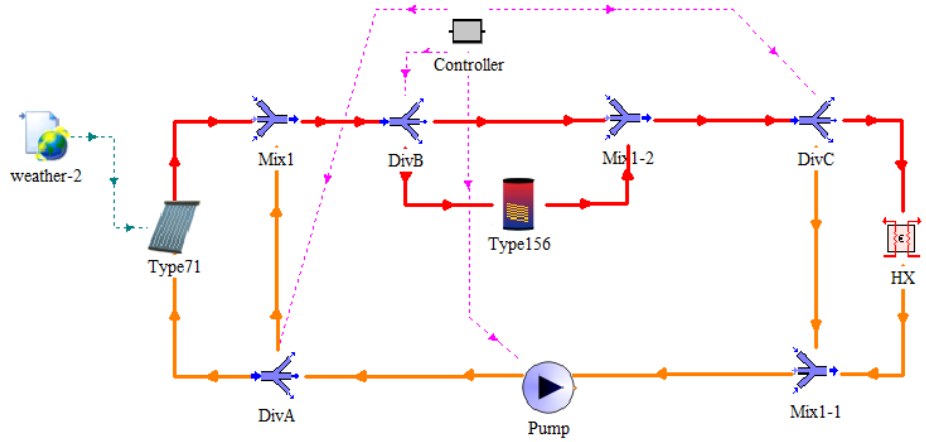

Figure 2. Numerical simulation model for scenario 1 and 2 (small-scale solar ORC with water tanks) developed in TRNSYS v18.

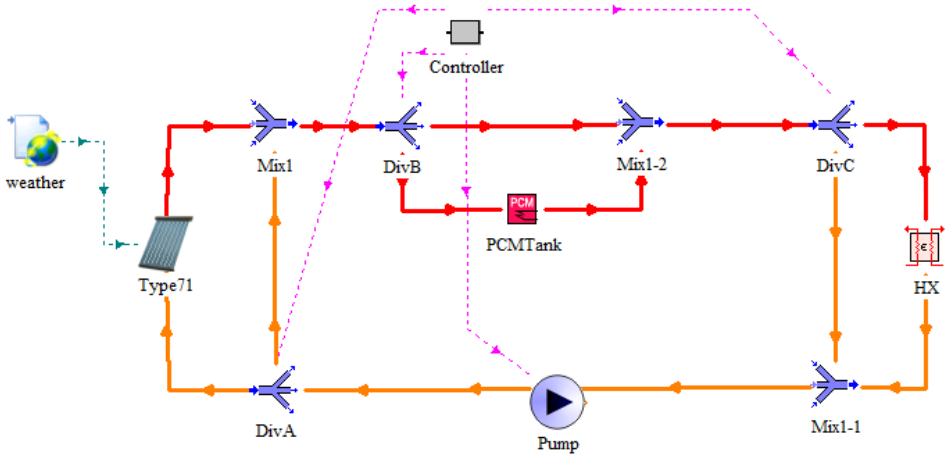

Figure 3. Numerical simulation model for scenario 3 (small-scale solar ORC with PCM tank) developed in TRNSYS v18.

Weather data were generated using Meteonorm and implemented within TRNSYS using the standard weather data reader component (Type 15-2). Seville was selected as a reference region for the simulation, with high solar availability (global average irradiance higher than 5.00 KWh/m^2 day) [28]. It is also characterised by a Mediterranean climate, with relatively mild winters and very warm summers.

Solar collectors were modelled using Type 71. This component simulates the thermal performance of a variety of evacuated tube collectors (ETC). Solar collector data from standard tests of efficiency was used for simulation. Technical parameters of the solar system are summarised in Table 2. Moreover, the hot media from the solar collectors to the evaporator of ORC is a mixture of water and 30% ethylene glycol.

Table 2. Characteristics of solar collector.

Parameters	Evacuated tube collectors (ETC)
Model	Vaillant VTK 1140
Number of collectors	4
Aperture area per collector (m^2)	2
Fluid specific heat (kJ/kg.K)	3.918
Tested flow rate (kg/h.m^2)	24 l/h/m^2
Optical efficiency (n_0)	0.642
Heat loss coefficient a_1 (W/m^2.K)	0.885
Heat loss coefficient a_2 (W/m^2.K^2)	0.001
Weight (when empty) (kg)	37
Stagnation temperature (ºC)	272
Collector slope (º)	37.23
TRNSYS Type	TYPE 71

As TES tanks, three alternatives are considered, whose technical parameters are defined in Table 1.

Water storage tanks were modelled using Type 156. They have a volume of 750 L, with a loss coefficient of 0.7/m^2K, according to reference commercial data. Heat loss rates of the modelled water tanks, considering 24h temperature decay with an ambient temperature of 20ºC, are 6.38 and 8.77 kWh/day for scenario 1 and 2, respectively. Stratification was considered through three tank nodes. The thermal energy storage capacity of the water tanks for a temperature difference of 20ºC is 17.3 kWh.

PCM tank was modelled through a new TRNSYS component. It is written in Fortran and compiled with the Fortran compiler. The developed model follows the structure of TRNSYS Type 156 based on a stratified fluid tank for sensible storage, in which sensible storage capacity was changed into latent heat storage. The latent heat performance is based on a mathematical procedure reported in the Report C5 of subtask C within the Task 32 of IEA Solar Heating and Cooling programme, about Simulation Models of PCM Storage Units [29], which has been tested and widely used in different PCM model proposals, such as the latent heat TES units based on PCM modules plunged into water tanks [30–32] or bulk PCM units [31,33]. This mathematical model is based on an enthalpy approach, in which the enthalpy is a continuous and invertible function of the temperature. It means that for a given volume and material, a continuous and reversible function can be calculated which will return the temperature (*T)* depending on the calculated enthalpy (*h)* [34].

Fig. 4 shows this function, which is modelled by a succession of three straight lines: two for the sensible heat in the solid and liquid phase, and one straight line in the phase change temperature region. This latent heat model requires six input parameters: specific heat capacity in solid and liquid stage (Cp_s and Cp_l, kJ/kg K), temperature range limit of phase change (T1 and T2, ºC), heat of fusion (h, kJ/kg) and average thermal conductivity (λ, W/m K). Subcooling has been neglected in material performance.

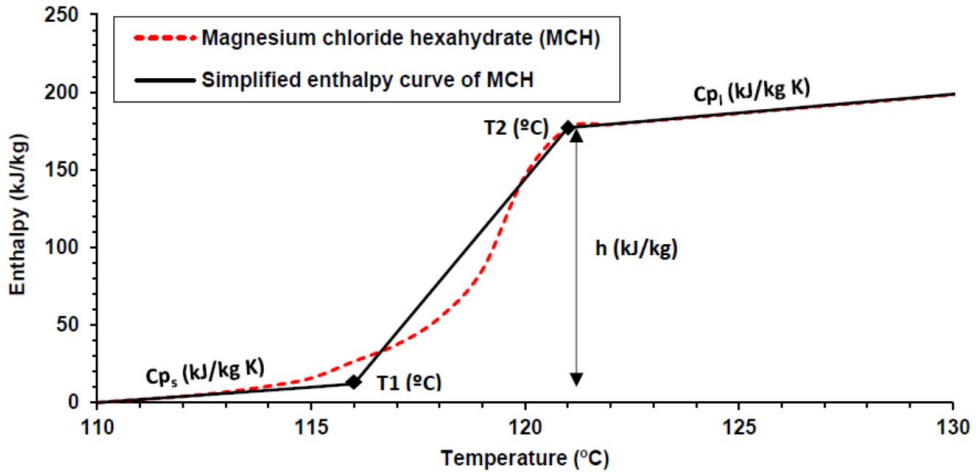

Figure 4. Characterization process of enthalpy curve implemented in new TRNSYS PCM type.

PCM selected for the latent heat storage unit is magnesium chloride hexahydrate (MCH, $MgCl_2 \cdot 6H_2O$), tanking as reference the comparative review developed by Lizana et al. [35,36]. Thermo-physical properties of the selected PCM are reported in Table 3 [37,38]. It consists of a salt hydrate, which has high latent heat capacity per unit volume, moderate thermal conductivity, and little volume change during melting [39]. The selected inorganic component is characterised by a melting temperature of 116 ºC, a heat storage capacity of 165kJ/kg and a PCM cost of approximately 0.50 €/kg [40].

Table 3. Thermo-physical properties of magnesium chloride hexahydrate (MCH, $MgCl_2 \cdot 6H_2O$). Properties (solid/liquid).

Properties	Characterisation
Melting temperature (ºC)	116
Latent heat (kJ/kg)	165
Thermal conductivity (W/m.K)	0.58-0.70
Specific heat (kJ/kg.K)	2.00/2.40
Density (kg/m^3)	1570/1450
Price (€/kg)	≈0.5

PCM tank is characterised by a volume of 200 L, with a loss coefficient of 0.7 W/m^2 K. Heat loss rate of modelled PCM tank is approximately 2.93 kWh/day, considering 24h temperature decay from 130ºC with an ambient temperature of 20ºC. Stratification was considered through three tank nodes. The thermal energy storage capacity of PCM unit for a temperature difference of 20ºC during the phase change temperature is 17.3 kWh.

Pump was modelled using Type 977, with a water flow of 320 kg/h. Other used components were diverting and mixing valves (Type 647 and 649), and different standard controllers and utilities.

The operation modes of the solar systems are three: solar energy storage in TES tank, direct solar energy to ORC heat exchanger (excess of solar heat) and indirect solar energy to ORC heat exchanger (heat provided by TES tank). They are illustrated in Fig. 5.

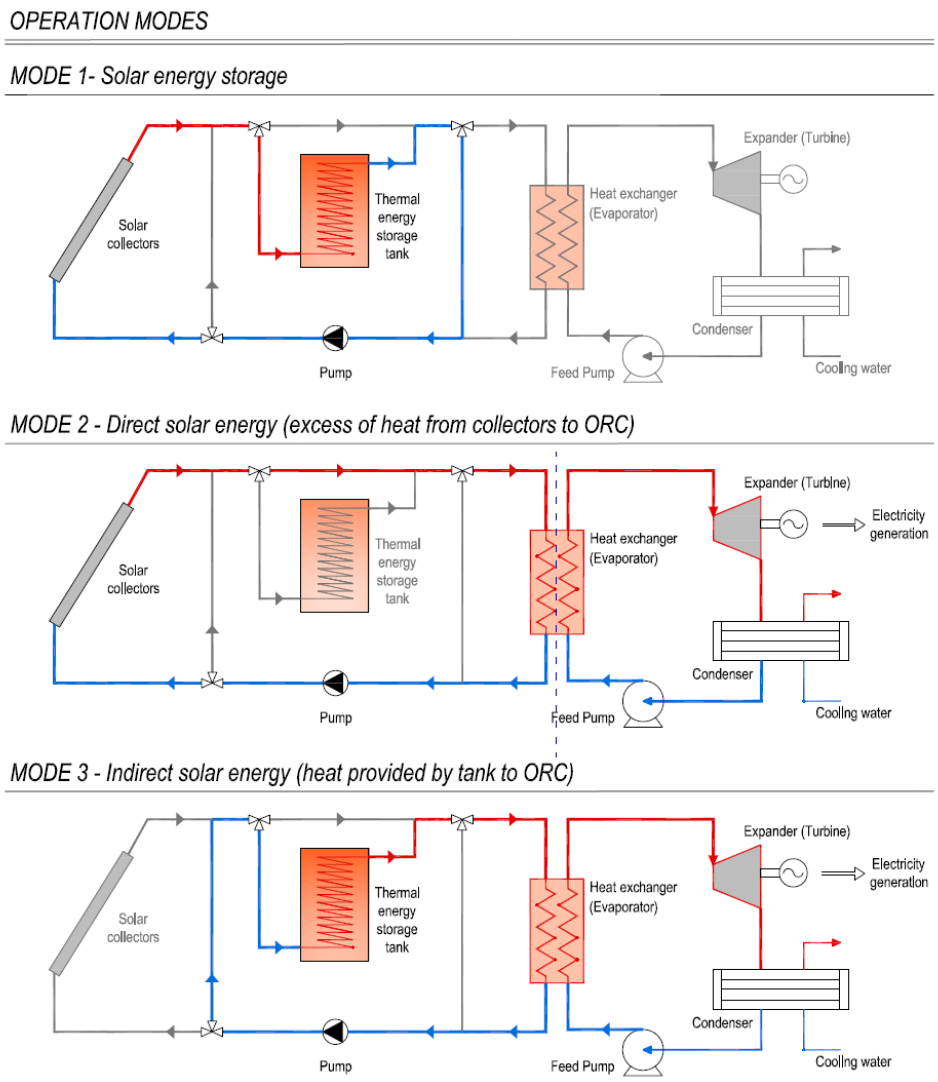

Figure 5. Operating modes of small-scale solar ORC system with TES.

Programming of operational strategies and priority of operating modes are summarized in Table 4. The controllers update each parameter along each simulation time step (3 minutes), changing operation mode according to operational strategies implemented. The operating modes operate sequentially, is not allowed to operate simultaneously.

Table 4. The linear operating structure of controllers.

Operating mode	Thermostats and controllers
Mode 1. Solar energy storage	Solar outlet - Upper dead-band dT: +10ºC (Type 2) Storage tank – T set-point 100ºC or 130ºC (Type 166)
Mode 2. Direct solar energy (Excess of solar heat to ORC)	Solar outlet - Upper dead-band dT: +10ºC (Type 2) Storage tank – Completely charged (Type 166)
Mode 3. Indirect solar energy (Heat provide by the tank to ORC)	Solar outlet - Temperature < 80ºC (Type 166) Storage tank – Temperature >80ºC or >110ºC (Type 166)

2.2. ORC model

One of the main effective parameters to run an ORC is the properties of available heat source such as temperature and mass flow rate. In this study, the solar heat from collectors (direct heat) and storage tanks (indirect heat), previously defined and characterised, provide the related inputs for the ORC simulation. Since properties of heat source change throughout the year, some adaptations of the ORC model are introduced to evaluate the seasonal performance in selected scenarios.

The selection of working fluid also has a great effect on the operation, efficiency and environmental impact of ORC. In this way, many aspects need to be taken into account, namely, thermodynamic properties, global warming potential (GWP), thermal stability, safety and environmental aspects, toxicity, flammability, auto-ignition temperature, costs, and availability, as it was discussed in several studies [3,41–44]. As a suitable working fluid for the cycle, with the mentioned heat source**,** isopentane was selected for the analysis of water-cooled ORC. In addition, the mixture of isopentane and isobutane at 50%wt was selected for air-cooled cycles.

The performance of ORC model is evaluated through three TES scenarios, considering all involved components from the heat exchanger (evaporator) for ASPEN simulation, as defined in Fig. 1. The seasonal boundary conditions for proposed scenarios, reported from TRNSYS simulation, are summarised in Table 5.

Table 5. Summary of mean operating conditions for ORC models.

Characterisation	**Scenario 1: Solar ORC – Water tank**	**Scenario 2: Solar ORC – Pressurised water tank**	**Scenario 3: Solar ORC - PCM tank**
Storage medium	Water	Pressurised water	Magnesium chloride hexahydrate
Mean temperature in the evaporator with direct heat (Solar heat from collectors)	147 ºC	136 ºC	137 ºC
Mean temperature in the evaporator with indirect heat (heat from storage tanks)	85 ºC	113 ºC	113 ºC
Hot source flow rate (kg/hr)	320 kg/hr	320 kg/hr	320 kg/hr

Monthly mean hot source temperature provided from solar panels ranges from 124 to 155 °C. Mean hot temperature in evaporator considering the proposed TES tanks are 85ºC, 113ºC and 113ºC for water tank, pressurised tank and PCM tank, respectively. The provided mass flow rate of the hot sources was equal to 320 kg/hr. Fig. 6 depicts a scheme of the ORC model in ASPEN. Taking into account reported boundary conditions, several ORC models were created at on-design conditions for the mentioned working temperatures.

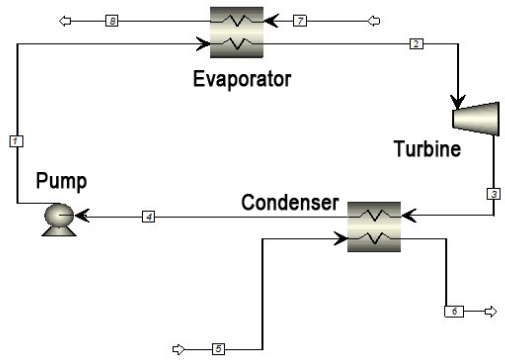

Figure 6. A schematic model of low-temperature ORC in ASPEN.

The following calculation assumptions were implemented in the ORC model: the mass flow of the working fluid and the cooling water is varied in order to match the 5 °C minimum temperature at the evaporator and the condenser, respectively; and the evaporating pressure was optimized in order to maximize the net power output of the plant.

The type of cooling system for ORC will depend on the available resources. Two concepts of cooling systems, namely water cooling and air cooling, were analysed. The water-cooled cycle was studied through two alternatives, one with a mean water temperature of 11 °C, which can be an option with cold underground water, and another one with a mean water supply temperature of 21ºC, as a reference value in the region under study. Moreover, the air-cooling concept was evaluated considering a mean ambient temperature of 20 °C, for scenarios in which water is not accessible. The related results give a better understanding of the effect of cooling properties on the cycle efficiency.

Overall, air coolers result in lower power generation and cycle efficiencies in comparison to water cooling at the same cooling temperatures and pressures. Based on the work of Rajabloo et. al. [27], in the case of air cooling, which requires high amounts of fan power, a mixture of the working fluid can be beneficial. As their results showed, temperature glide at condenser leads to lower required mass flow rate of air and less fan power consumption consequently. However, all possible alternatives are considered for solar-ORC implementation in this work.

3. Results and discussions

3.1. Solar energy availability through TES alternatives

Monthly solar energy availability for solar ORC with three TES alternatives are shown in Tables 6-8, and annual performance with regard to final energy balance and operating temperature ranges are compared in Fig. 7 and Table 9.

Table 6 summaries the results of the monthly performance of the direct and indirect solar heat in **Scenario 1 (Solar ORC with water tank)**.

Table 6. Monthly performance of the direct and indirect solar energy availability for ORC unit with water tank.

Month	Total solar radiation (kWh)	Useful collector gain (kWh)	Heat provided by tank to ORC (kWh)	Mean temperature[a] (ºC)	Excess of heat from collector to ORC (kWh)	Mean temperature[a] (ºC)	Water tank losses (kWh)
January	1034	610	299	84	104	135	157
February	1016	599	348	84	100	140	152
March	1430	853	384	85	300	153	170
April	1326	774	390	85	223	155	165
May	1529	892	418	85	300	153	173
June	1513	879	416	85	299	149	168
July	1689	996	447	85	377	152	174
August	1606	958	447	85	342	151	174
September	1490	895	418	85	311	154	167
October	1272	762	384	85	212	147	169
November	898	521	294	84	70	141	159
December	916	530	296	85	78	140	163
Total/Mean	15720	9270	4539	mean: 85	2716	mean: 147	1990

[a] Mean temperature in the evaporator under the same boundary conditions in all scenarios.

This water storage scenario results in a seasonal collector efficiency of 59%. Water tank stores 71% of useful collector gains, of which 49% is provided with an average supply temperature in the evaporator of 85ºC. The water tank is also characterised by a high percentage of heat losses (21%), associated with the large tank size in comparison with PCM tank.

Table 7 summaries the results of the monthly performance of the direct and indirect solar heat in **Scenario 2 (Solar ORC with pressurised water tank)**.

Table 7. Monthly performance of the direct and indirect solar energy availability for ORC unit with pressurised water tank.

Month	Total solar radiation (kWh)	Useful collector gain (kWh)	Heat provided by tank to ORC (kWh)	Mean temperature[a] (ºC)	Excess of heat from collector to ORC (kWh)	Mean temperature[a] (ºC)	Water tank losses (kWh)
January	1034	598	239	113	61	129	220
February	1016	585	302	112	64	128	217
March	1430	842	358	113	240	143	243
April	1326	762	349	113	175	140	236
May	1529	881	398	113	235	139	246
June	1513	870	397	113	233	135	239
July	1689	987	430	113	308	139	248
August	1606	949	424	113	277	139	247
September	1490	886	407	114	240	140	238
October	1272	750	339	113	167	138	243
November	898	507	239	112	39	131	228
December	916	518	259	113	31	126	234
Total/Mean	15720	9133	4142	mean: 113	2070	mean: 136	2840

[a] In evaporator under the same boundary conditions in all scenarios.

The pressurised water tank results in a seasonal collector efficiency of 58%, derived from the higher operating temperature. Pressurised water tank stores 77% of useful collector gains, of which 45% is provided with an average supply temperature in the evaporator of 113ºC. The pressurised tank is also characterised by a high percentage of heat losses (31%), associated with the large tank size in comparison with PCM tank, and the higher storage temperature in comparison with scenario 1.

Table 8 summaries the results of the monthly performance of the direct and indirect solar heat of integration **in Scenario 3 (Solar ORC with PCM tank)**.

Table 8. Monthly performance of the direct and indirect solar energy availability for ORC unit with PCM tank.

Month	Total solar radiation (kWh)	Useful collector gain (kWh)	Heat provided by tank to ORC (kWh)	Mean temperature[a] (ºC)	Excess of heat by collector to ORC (kWh)	Mean temperature[a] (ºC)	PCM Tank losses (kWh)
January	1034	585	343	113	119	144	79
February	1016	583	376	113	107	129	74
March	1430	840	420	113	307	142	83
April	1326	760	413	113	237	138	80
May	1529	876	450	113	308	140	84
June	1513	863	443	113	309	137	81
July	1689	985	481	113	384	140	84
August	1606	947	480	113	351	139	84
September	1490	884	454	113	318	140	81
October	1272	747	415	113	220	138	82
November	898	503	320	113	78	129	77
December	916	518	327	113	85	124	79
Total/Mean	15720	9090	4921	mean: 113	2823	mean: 137	968

[a] In evaporator under the same boundary conditions in all scenarios.

This integration shows the same seasonal collector efficiency than pressurised water tank (58%), derived from the same operating temperature, between 110 ºC and 130ºC. PCM tank stores 70% of useful collector gains, of which 54% is provided with an average supply temperature in the evaporator of 113ºC. PCM tank is also characterised by a low percentage of heat losses (11%), associated with the smaller tank size in comparison with water tanks.

Fig. 7 compares the annual solar energy balance in three solar ORC scenarios, and Table 9 summaries the results of final energy balance and operating temperatures. Operating temperatures were analysed according to the temperature evolution during discharging periods in evaporator, with the calculation of mean temperature value, standard deviation (SD), 25th percentile and 75th percentile.

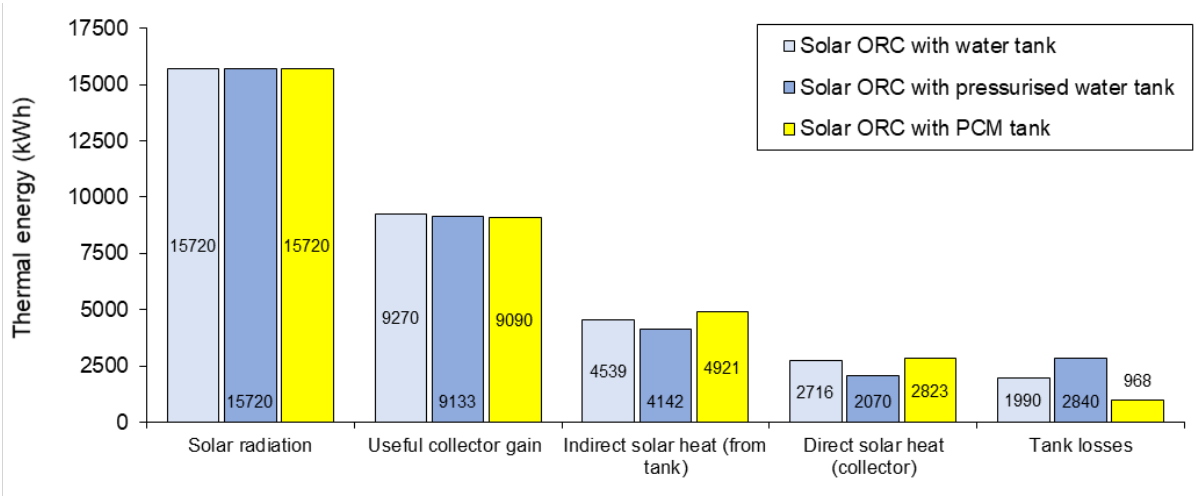

Figure 7. Comparison of annual thermal energy availability of solar ORC schemes with water tanks and PCM tank.

Table 9. Summary of results in three solar TES scenarios.

Performance indicators	**Scenario 1: Solar ORC – Water tank**	**Scenario 2: Solar ORC – Pressurised water tank**	**Scenario 3: Solar ORC - PCM tank**
Storage medium	Water	Pressurised water	MCH
Performance of solar collectors			
Useful collector gain	9270 kWh (100%)	9133 kWh (100%)	9090 kWh (100%)
Seasonal collector efficiency	59%	58%	58%
Useful solar heat (direct and indirect)	7255 kWh (78%) [a]	6211 kWh (68%) [a]	7745 kWh (85%) [a]
Energy balance of TES tanks			
Indirect useful heat (heat provided by tank)	4539 kWh (49%) [a]	4142 kWh (45%) [a]	4921 kWh (54%) [a]
Tank losses	1990 kWh (21%) [a]	2840 kWh (31%) [a]	968 kWh (11%) [a]
Temperature evaluation in the evaporator (during discharge) [b]			
Average evaporator temperature ºC	85 ºC	113 ºC	113 ºC
Standard deviation (SD)	5	5	3
25th percentile	80 ºC	109 ºC	111 ºC
75th percentile	89 ºC	117 ºC	114 ºC

[a] Percentages calculated in relation with useful collector gains.
[b] Comparison of temperatures in the evaporator under the same boundary conditions in all scenarios.

The results show that PCM tank has higher benefits in comparison with water tank assemblies to enhance solar ORC performance. PCM tank can provide a higher capacity of useful solar heat in comparison with a pressurised water tank (+25%) and conventional hot water tank (+7%), with small heat losses of 11%, Heat losses are reduced by more than 50% in comparison with sensible heat storage alternatives. In addition, the annual mean temperature in the evaporator for ORC cycle is higher than conventional water tank assembly, and within a higher and narrower output temperature range than with a pressurised water tank, which enhances final ORC cycle efficiency. The temperature in evaporator during 50% of discharge time ranges between 111ºC and 114 ºC for PCM tank, between 109ºC and 117ºC for pressurised water tank

and between 80ºC and 89ºC for conventional water tank. Final useful solar heat availability of three solar storage scenarios, considering direct and indirect energy supply in comparison with useful collector gains, is 78%, 68% and 85%, for water, pressurised water and PCM, respectively. These results allow highlighting the potential benefits that latent heat integration provides to improve the ORC performance using solar energy.

3.2. Electricity availability of ORC through TES alternatives

The results of ORC models carried out in ASPEN according to the boundary conditions reported from TRNSYS simulations for Scenario 1 (Solar ORC – Water tank) and Scenario 2 (Solar ORC - PCM tank) are summarised in Tables 10-12. The ORC models consider an average direct and indirect solar source temperatures according to the results previously provided in Table 6, 7 and 8.

Table 10 shows the performance of ORC water-cooled model for **Scenario 1 (Solar ORC – Water tank)** with a parametric analysis concerning the evaporation pressure. It only considers the use of indirect heat from the storage tank with a mean hot source temperature in the evaporator of 85 °C and cooling water at 11 °C.

Table 10. Results of water-cooled ORC with $T_{hot\ source}$ = 85 °C, $T_{cold\ water}$ = 11 °C, P_{cond} = 2.7 bar, and, $M_{hot\ source}$ = 320 kg/hr

$P_{evap.}$ (bar)	W_{net} (kW)	$Q_{in,evap}$ (kW)	Efficiency (%)	$T_{out,evap}$ (°C)
11.0	586	5285	11.09	70.8
10.9	613	5568	11.01	70.0
10.0	774	7390	10.48	65.1
9.0	938	9596	9.77	59.2
8.0	1043	11645	8.95	53.6
7.0	1104	13814	7.99	47.8
6.0	1097	16074	6.82	41.7

The results show that although optimum net power occurs at 7 bar, the return temperature was too low. The recoverable heat duty and evaporation pressure have a constraint on the return temperature, which should be higher than 70 °C to have stable functionality of the storage tank. The optimum achievable evaporation pressure was 10.85 bar for the hot source temperature of 85 °C, which provides a final ORC efficiency higher than 11%. Therefore, the optimum evaporation pressure and heat duty are implemented in this margin.

The same boundaries were applied to the ORC model with a hot temperature of 113 °C, associated with **Scenario 2 and 3 (indirect heat from pressurised water tank and PCM tank)**, and considering an average temperature in the evaporator of 130ºC, as a reference value for **direct solar heating in three scenarios**. In addition, as a conservative value of water-cooled cycle, the model was run with a mean water supply temperature of 21 °C, as a reference value in the region under study. The results at optimum evaporation pressure regarding solar tank constraints are available in Table 11.

Table 11. Results of water-cooled ORC with $T_{cold\ water}$ = 21 °C, P_{cond} = 3.7 bar, and, $M_{hot\ source}$ = 320 kg/hr

Hot source temperature (°C)	$P_{evap.}$ (bar)	W_{net} (W)	$Q_{in,evap}$ (W)	Thermal efficiency (%)
85	10.9	498.4	5597.9	8.9
113	13.6	1682.7	16049.7	10.5
130	16.8	2637.5	22462.1	11.7

This parametric analysis, with the optimum evaporation pressure for each scenario, highlights that with higher hot source temperature and higher evaporation pressures, higher net generated power and cycle efficiencies are obtained, ranging for Scenario 1 (Water tank) from 8.9 to 11.7%, and for Scenario 2 and 3 (Pressurised water tank and PCM tank) from 10.5 to 11.7%. Comparing the ORC operation by indirect heat from TES tanks, the results show that pressurised water and latent heat storage can increase the ORC efficiency by up to 18% (from 8.9% to 10.5%) and the net generated power from 498.4W to 1682.7W, scaled up by 238%.

The air-cooling possibility for ORC working with the same working fluid and heat resource properties was investigated, with a mean ambient temperature at the studied zone of 20 °C. Moreover, the possibility of air cooling of ORC was also studied by implementing a mixture of isobutane and isopentane at 50%wt as working fluid. The results are available in Table 12.

Table 12. Results of air-cooled ORC with T_{air} = 20 °C, P_{cond} = 2.3 bar, and, $M_{hot\ source}$ = 320 kg/hr

Hot source temperature (°C)	$P_{evap.}$ (bar)	W_{net} (W)	$Q_{in,evap}$ (W)	Thermal efficiency (%)
85 (pure working fluid)	-	-	-	-
85 (mixture working fluid)	7.2	389.3	5577.6	7.0
113 (pure working fluid)	13.73	1721.92	15800	10.9
113 (mixture working fluid)	8.89	1589.6	15791.9	10.1
130 (pure working fluid)	17	2695.3	22181.1	12.1
130 (mixture working fluid)	10.4	2437.4	22164.5	11.0

Since the mixture of working fluids causes temperature glide during the evaporation and condensation, evaporation pressures were less. Hence, less power was generated in the turbine leading to fewer cycle efficiencies. It should be also considered that despite reduced efficiencies by using air-cooled ORC, the higher working temperature of PCM tank provides higher efficiencies throughout the operation.

3.3. Economic analysis

The total investment cost of three proposed small-scale solar ORC alternatives are evaluated as shown in Table 13, using cost data gathered from different cost database [45–47], market survey and scientific publications.

Table 13. Cost analysis of the different integrations for small-scale solar ORC system.

Elements	Scenario 1. Solar ORC – Water tank	Scenario 2: Solar ORC – Pressurised water tank	Scenario 3: Solar ORC - PCM tank
Solar collectors (8m^2 of ETC)	6360€	6360€	6360€
TES tank	2300€ (750dm^3)	3000€ (750dm^3)	1500€ (200dm^3)
ORC system (≈2kW)	10000€	10000€	10000€
Additional elements	1800€	1800€	1800€
Total cost	**18660€**	**19360€**	**17860€**

Solar collectors based on ETC costs 6360€, with a specific cost ratio of approximately 795€/m^2, higher than flat plate collectors situated in 260€/m^2 [47]. In this case, as temperatures higher than 130 ºC are needed, ETC was selected instead of flat plate collectors to increase the seasonal efficiency of the system, increasing the final cost.

The investment cost of the water tank and pressurised water tank, for a tank size of 750dm^3, is approximately 2300€ and 3000€, respectively [47]. The higher cost of scenario 2 is mainly associated with the need for pressure requirements higher than 5 bar in order to remain water in liquid phase up to 150ºC [48,49]. In the case of PCM tank, the investment cost is reduced due to a smaller size of 200dm^3. However, it has additional requirements in comparison with a water tank, associated with the need for a higher heat transfer ratio between the PCM and the heat transfer fluid [50], corrosion protection for the specific use of salt hydrates [51] and the PCM cost, which in this case is quite competitive, approximately 0.50 €/kg [40]. This configuration results in a PCM tank very competitive in comparison with water scenarios, with a reduction of investment cost by 35% and 50% compared to the water tank and pressurised water tank, respectively.

In the case of ORC unit, the specific cost (€/kW) for small-scale applications is still too high [52]. The specific cost of ORC units is hardly below 5000 €/kW for power sizes below 10 kW [8]. Previous studies showed an investment cost ratio of 5000 €/kW [53], 5775 €/kW [54] and 5833 €/kW [15]. According to Tocci et al. [52], the specific cost of ORC should not exceed the value of 3500€/kW in the power range below 10kW to consider it competitive. The remaining cost is related to piping, insulation, instrumentation and control, structures and other utilities.

Fig. 8 shows a sensitivity analysis of the investment cost of three ORC solutions studied in this work, considering a potential deviation of ±20% for different elements.

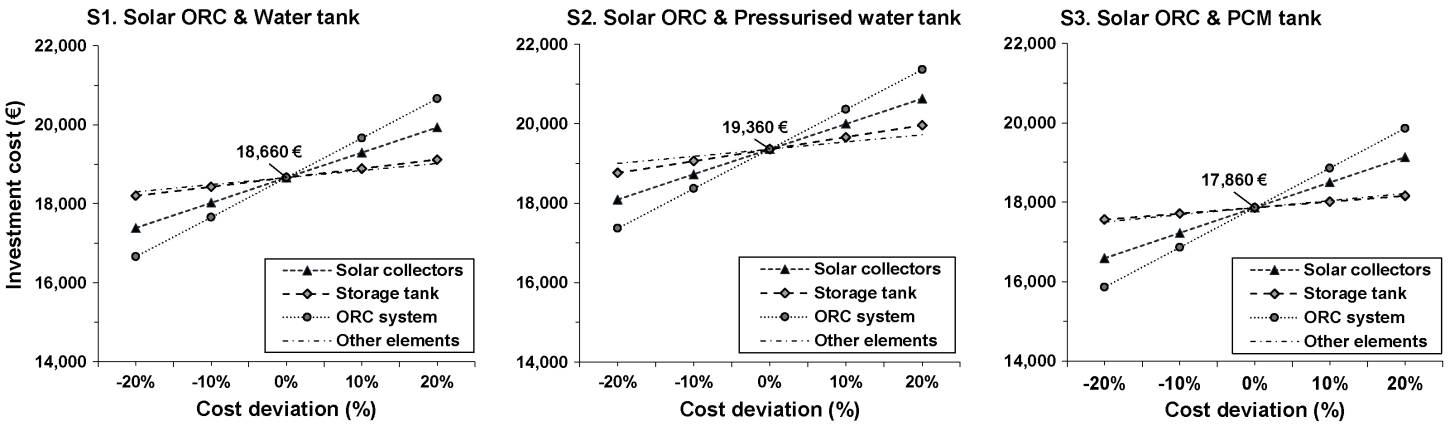

Figure 8. Sensitivity analysis of the investment cost of three proposed small-scale solar ORC scenarios.

The results show that the total investment costs for scenario 1, 2 and 3 are 18660€, 19360€ and 17860€, respectively. Scenario 2 shows an increase in investment cost by 4% compared to a conventional water tank due to the pressure requirements. PCM integration shows the benefits of reduced tank size and low-cost of selected PCM, which reduces the final investment cost of solar ORC assembly by 4% and 8%, in comparison with water tank and pressurised water tank, respectively. Additionally, with a more competitive ORC technology, with a cost deviation of -20%, final investment cost could be reduced below 16000€ in scenario 3. However, special attention should be paid to PCM cost and heat exchanger elements between PCM and heat exchanger fluid to ensure appropriate performance.

The results highlight the potential benefits of using latent heat storage to enhance ORC performance, providing higher and narrower output temperature ranges and higher thermal energy storage capacity, with a reduction of heat losses and an investment cost reduction of the storage tank by more than 35% in comparison with water storage scenarios. Furthermore, at the water-scarce situation, air coolers are feasible based on this study.

4. Conclusions

This paper evaluates the potential application of a latent heat storage unit to enhance solar ORC performance in comparison with previous schematic assemblies, at operating temperatures between 80ºC and 140ºC, adequate for low-cost non-concentrating solar-thermal collectors. The simulation was carried out through two models, developed in TRNSYS for solar energy balance, and ASPEN for ORC performance. Based on the evaluation of the proposed solar ORC integrations, it is possible to extract the following conclusions:

The integration of a solar PCM tank into an ORC system can provide 54% of useful collector gains as indirect heat, with a higher and narrower temperature range in the evaporator of approximately 113ºC, increasing the solar thermal energy capacity by 19%, reducing heat losses in storage tank by 66% and decreasing the investment cost by 50%, in comparison with the pressurised water tank assembly under the same boundary conditions. PCM effectively enhances the potential of solar energy sources for electricity generation by small-scale ORC systems in domestic facilities, increasing the useful solar heat availability from 68% to 85%, with regards to useful collector gains.

The operating temperatures and storage capacity of the storage tanks considerably affect the overall performance of the solar ORC system. The results show that latent heat storage can increase the ORC efficiency up to approximately 18% (from 8.9% to 10.5%) and the net generated power scaled up by 238% (from 498.4 to 1682.7W) in comparison with a conventional water tank assembly. Furthermore, water-cooled ORC has showed higher net power in comparison with the air-cooled one. This is because fan power consumption at air-cooled ORC is considerable, which leads to less net generated power. Besides, at the water-scarce situation, air coolers are feasible based on this study.

Latent heat storage based on magnesium chloride hexahydrate is highlighted as a potential storage solution to enhance the performance of solar ORC integration at appropriate temperatures for low-cost non-concentrating solar-thermal collectors. The results highlight the potential benefits of this PCM in comparison with water tank assemblies.

Acknowledgements

This work was made possible thanks to the YEAR Network (European Young Associated Researchers), through the First international prize YEAR AWARD 2018, to the best research project idea during the YEAR Network Conference in Vienna (Austria).

References

[1] B.F. Tchanche, G. Papadakis, G. Lambrinos, A. Frangoudakis, Fluid selection for a low-temperature solar organic Rankine cycle, Applied Thermal Engineering. 29 (2009) 2468–2476. doi:10.1016/j.applthermaleng.2008.12.025.

[2] D. Tiwari, A.F. Sherwani, D. Atheaya, A. Kumar, N. Kumar, Thermodynamic analysis of Organic Rankine cycle driven by reversed absorber hybrid photovoltaic thermal compound parabolic concentrator system, Renewable Energy. 147 (2019) 2118–2127. doi:10.1016/j.renene.2019.10.018.

[3] O. Aboelwafa, S.E.K. Fateen, A. Soliman, I.M. Ismail, A review on solar Rankine cycles: Working fluids, applications, and cycle modifications, Renewable and Sustainable Energy Reviews. 82 (2018) 868–885. doi:10.1016/j.rser.2017.09.097.

[4] J. Freeman, I. Guarracino, S.A. Kalogirou, C.N. Markides, A small-scale solar organic Rankine cycle combined heat and power system with integrated thermal energy storage, Applied Thermal Engineering. 127 (2017) 1543–1554. doi:10.1016/j.applthermaleng.2017.07.163.

[5] H. Zhai, Q. An, L. Shi, V. Lemort, S. Quoilin, Categorization and analysis of heat sources for organic Rankine cycle systems, Renewable and Sustainable Energy Reviews. 64 (2016) 790–805. doi:10.1016/j.rser.2016.06.076.

[6] J.S. Pereira, J.B. Ribeiro, R. Mendes, G.C. Vaz, J.C. André, ORC based micro-cogeneration systems for residential application

- A state of the art review and current challenges, Renewable and Sustainable Energy Reviews. 92 (2018) 728–743. doi:10.1016/j.rser.2018.04.039.

[7] T. Tartière, M. Astolfi, A World Overview of the Organic Rankine Cycle Market The Overview the Organic Rankine Assessing the feasibility of the heat, Energy Procedia. 129 (2017) 2–9. doi:10.1016/j.egypro.2017.09.159.

[8] S. Quoilin, M. Van Den Broek, S. Declaye, P. Dewallef, V. Lemort, Techno-economic survey of Organic Rankine Cycle (ORC) systems, Renewable and Sustainable Energy Reviews. 22 (2013) 168–186. doi:10.1016/j.rser.2013.01.028.

[9] K. Rahbar, S. Mahmoud, R.K. Al-Dadah, N. Moazami, S.A. Mirhadizadeh, Review of organic Rankine cycle for small-scale applications, Energy Conversion and Management. 134 (2017) 135–155. doi:10.1016/j.enconman.2016.12.023.

[10] D. Manolakos, G. Papadakis, S. Kyritsis, K. Bouzianas, Experimental evaluation of an autonomous low-temperature solar Rankine cycle system for reverse osmosis desalination, Desalination. 203 (2007) 366–374. doi:10.1016/j.desal.2006.04.018.

[11] X.D. Wang, L. Zhao, J.L. Wang, W.Z. Zhang, X.Z. Zhao, W. Wu, Performance evaluation of a low-temperature solar Rankine cycle system utilizing R245fa, Solar Energy. 84 (2010) 353–364. doi:10.1016/j.solener.2009.11.004.

[12] E.H.M. Kane, D. Favrat, Intégration et optimisation thermoéconomique & environomique de centrales thermiques solaires hybrides, Ecole polytechnique Fédérale de Lausanne, Lausanne, 2002.

[13] J. Freeman, K. Hellgardt, C.N. Markides, An assessment of solar-powered organic Rankine cycle systems for combined heating and power in UK domestic applications, Applied Energy. 138 (2015) 605–620. doi:10.1016/j.apenergy.2014.10.035.

[14] S. Quoilin, M. Orosz, H. Hemond, V. Lemort, Performance and design optimization of a low-cost solar organic Rankine cycle for remote power generation, Solar Energy. 85 (2011) 955–966. doi:10.1016/j.solener.2011.02.010.

[15] F. Calise, M.D. D'Accadia, M. Vicidomini, M. Scarpellino, Design and simulation of a prototype of a small-scale solar CHP system based on evacuated flat-plate solar collectors and Organic Rankine Cycle, Energy Conversion and Management. 90 (2015) 347–363. doi:10.1016/j.enconman.2014.11.014.

[16] Li Gang, Energy and exergy performance assessments for latent heat thermal energy storage systems, Renewable and Sustainable Energy Reviews. 51 (2015) 926–954. doi:10.1016/j.rser.2015.06.052.

[17] R. murthy B.V., V. Gumtapure, Thermal property study of fatty acid mixture as bio-phase change material for solar thermal energy storage usage in domestic hot water application, Journal of Energy Storage. 25 (2019) 100870. doi:10.1016/j.est.2019.100870.

[18] M. He, L. Yang, W. Lin, J. Chen, X. Mao, Z. Ma, Preparation, thermal characterization and examination of phase change materials (PCMs) enhanced by carbon-based nanoparticles for solar thermal energy storage, Journal of Energy Storage. 25 (2019) 100874. doi:10.1016/j.est.2019.100874.

[19] H. Mousa, J. Naser, O. Houche, Using PCM as energy storage material in water tanks: Theoretical and experimental investigation, Journal of Energy Storage. 22 (2019) 1–7. doi:10.1016/j.est.2019.01.018.

[20] P.B. Salunkhe, D. Jaya Krishna, Investigations on latent heat storage materials for solar water and space heating applications, Journal of Energy Storage. 12 (2017) 243–260. doi:10.1016/j.est.2017.05.008.

[21] K. Bhagat, S.K. Saha, Numerical analysis of latent heat thermal energy storage using encapsulated phase change material for solar thermal power plant, Renewable Energy. 95 (2016) 323–336. doi:10.1016/j.renene.2016.04.018.

[22] S.C. Costa, K. Mahkamov, M. Kenisarin, K. Lynn, E. Halimic, D. Mullen, Solar salt latent heat thermal storage for a small solar organic rankine cycle plant, ASME 2018 12th International Conference on Energy Sustainability, ES 2018, Collocated with the ASME 2018 Power Conference and the ASME 2018 Nuclear Forum. (2018) 1–10.

[23] L. Cioccolanti, R. Tascioni, A. Arteconi, Mathematical modelling of operation modes and performance evaluation of an innovative small-scale concentrated solar organic Rankine cycle plant, Applied Energy. 221 (2018) 464–476. doi:10.1016/j.apenergy.2018.03.189.

[24] J. Lizana, R. Chacartegui, A. Barrios-Padura, C. Ortiz, Advanced low-carbon energy measures based on thermal energy storage in buildings: A review, Renewable and Sustainable Energy Reviews. 82 (2018) 3705–3749. doi:10.1016/j.rser.2017.10.093.

[25] TRNSYS v18. A transient system simulation program, (n.d.).

[26] Aspen Plus, (n.d.). https://www.aspentech.com/products/engineering/aspen-plus/ (accessed May 13, 2019).

[27] T. Rajabloo, P. Iora, C. Invernizzi, Mixture of working fluids in ORC plants with pool boiler evaporator, Applied Thermal Engineering. 98 (2016) 1–9. doi:10.1016/j.applthermaleng.2015.10.159.

[28] J.M. Sancho Ávila, J. Riesco Martín, C. Jiménez Alonso, M.C. Sanchez de Cos Escuin, J. Mortero Cadalso, M. López Bartolomé, Atlas de Radiación Solar en España utilizando datos del SAF de Clima de EUMETSAT, Agencia Estatal de Meteorología. Ministerio de Agricultura, Alimentación y Medio ambiente, 2012.

[29] W. Streicher, J. Bony, S. Citherlet, A. Heinz, P. Puschnig, H. Schranzhofer, J.M. Schultz, Simulation models of PCM storage units. A Report of IEA Solar Heating and Cooling programme - Task 32 "Advanced storage concepts for solar and low energy buildings". Report C5 of Subtask C, 2008. http://ww.iea-shc.org/publications/downloads/task32-c5.pdf.

[30] J. Bony, S. Citherlet, Numerical model and experimental validation of heat storage with phase change materials, Energy and Buildings. 39 (2007) 1065–1072. doi:10.1016/j.enbuild.2006.10.017.

[31] J. Bony, M. Ibáñez, P. Puschnig, S. Citherlet, L. Cabeza, A. Heinz, Three different approaches to simulate PCM bulk elements in a solar storage tank, in: Proc. of 2nd Conference on Phase Change Material and Slurry, Yverdon-les-Bains, 2005.

[32] J. Bony, S. Citherlet, Comparison between a new trnsys model and experimental data of phase change materials in a solar combisystem, Building & Simulation Conference. (2007) 371–378.

[33] P. Puschnig, A. Heinz, W. Streicher, TRNSYS simulation model for an energy storage for PCM slurries and/or PCM modules, in: Proc. of 2nd Conference on Phase Change Material and Slurry, Yverdon-les-Bains, 2005.

[34] J. Lizana, D. Friedrich, R. Renaldi, R. Chacartegui, Energy flexible building through smart demand-side management and latent heat storage, Applied Energy. 230 (2018) 471–485. doi:10.1016/j.apenergy.2018.08.065.

[35] J. Lizana, R. Chacartegui, A. Barrios-Padura, J.M. Valverde, Advances in thermal energy storage materials and their applications towards zero energy buildings: A critical review, Applied Energy. 203 (2017) 219–239. doi:10.1016/j.apenergy.2017.06.008.

[36] J. Lizana, R. Chacartegui, A. Barrios-Padura, J.M. Valverde, C. Ortiz, Identification of best available thermal energy storage compounds for low-to-moderate temperature storage applications in buildings, Materiales de Construcción. 68 (2018) 1–35. doi:https://doi.org/10.3989/mc.2018.10517.

[37] H. Mehling, L.F. Cabeza, Solid-liquid phase change materials, in: Heat and Cold Storage with PCM. An up to Date Introduction into Basics and Applications., Springer, 2008: pp. 11–55.

[38] S. Cantor, DSC study of melting and solidification of salt hydrates, Thermochimica Acta. 33 (1979) 69–86. doi:10.1016/0040-6031(79)87030-6.

[39] T. Khadiran, M.Z. Hussein, Z. Zainal, R. Rusli, Advanced energy storage materials for building applications and their thermal performance characterization: A review, Renewable and Sustainable Energy Reviews. 57 (2016) 916–928. doi:10.1016/j.rser.2015.12.081.

[40] V. Mamani, A. Gutiérrez, S. Ushak, Development of low-cost inorganic salt hydrate as a thermochemical energy storage material, Solar Energy Materials and Solar Cells. 176 (2018) 346–356. doi:10.1016/j.solmat.2017.10.021.

[41] T. Rajabloo, D. Bonalumi, P. Iora, Effect of a partial thermal decomposition of the working fluid on the performances of ORC power plants, Energy. 133 (2017) 1013–1026. doi:10.1016/j.energy.2017.05.129.

[42] A. Uusitalo, J. Honkatukia, T. Turunen-Saaresti, A. Grönman, Thermodynamic evaluation on the effect of working fluid type and fluids critical properties on design and performance of Organic Rankine Cycles, Journal of Cleaner Production. 188 (2018) 253–263. doi:10.1016/j.jclepro.2018.03.228.

[43] E. Saloux, M. Sorin, H. Nesreddine, A. Teyssedou, Reconstruction procedure of the thermodynamic cycle of organic Rankine cycles (ORC) and selection of the most appropriate working fluid, Applied Thermal Engineering. 129 (2018) 628–635. doi:10.1016/j.applthermaleng.2017.10.077.

[44] A.I. Papadopoulos, M. Stijepovic, P. Linke, On the systematic design and selection of optimal working fluids for Organic Rankine Cycles, Applied Thermal Engineering. 30 (2010) 760–769. doi:10.1016/j.applthermaleng.2009.12.006.

[45] BEDEC. Instituto de Tecnología de la Construcción de Cataluña - ITeC, (n.d.). http://itec.es/noubedec.e/bedec.aspx (accessed November 9, 2016).

[46] PREOC 2016. Precios de edificación y obra civil en España, (2016). http://www.preoc.es.

[47] Generador de precios de la construcción. España. CYPE Ingenieros, S.A., (n.d.). http://www.generadordeprecios.info/ (accessed November 9, 2016).

[48] E. Bellos, C. Tzivanidis, K.A. Antonopoulos, Exergetic, energetic and financial evaluation of a solar driven absorption cooling system with various collector types, Applied Thermal Engineering. 102 (2016) 749–759. doi:10.1016/j.applthermaleng.2016.04.032.

[49] C. Kutlu, J. Li, Y. Su, G. Pei, S. Riffat, Off-design performance modelling of a solar organic Rankine cycle integrated with pressurized hot water storage unit for community level application, Energy Conversion and Management. 166 (2018) 132–145. doi:10.1016/j.enconman.2018.04.024.

[50] R. Padovan, Analysis and optimization of PCM enhanced storage tanks for Solar Domestic Hot Water systems, Università degli Studi di Udine, 2014. doi:10.1016/j.solener.2013.12.034.

[51] S. Höhlein, A. König-Haagen, D. Brüggemann, Macro-encapsulation of inorganic phase-change materials (PCM) in metal capsules, Materials. 11 (2018). doi:10.3390/ma11091752.

[52] L. Tocci, T. Pal, I. Pesmazoglou, B. Franchetti, Small scale Organic Rankine Cycle (ORC): A techno-economic review, Energies. 10 (2017). doi:10.3390/en10040413.

[53] L. Cioccolanti, R. Tascioni, E. Bocci, M. Villarini, Parametric analysis of a solar Organic Rankine Cycle trigeneration system for residential applications, Energy Conversion and Management. 163 (2018) 407–419. doi:10.1016/j.enconman.2018.02.043.

[54] B.F. Tchanche, S. Quoilin, S. Declaye, G. Papadakis, V. Lemort, Economic feasibility study of a small scale organic rankine cycle system in waste heat recovery application, ASME 2010 10th Biennial Conference on Engineering Systems Design and Analysis, ESDA2010. 1 (2010) 249–256. doi:10.1115/ESDA2010-24828.